31. Van Den Born J, Van Den Heuvel LP, Bakker MA *et al*. A monoclonal antibody against GBM heparan sulfate induces an acute selective proteinuria in rats. *Kidney Int* 1992; 41: 115–123
32. Bertolatus JA, Klinzman D. Macromolecular sieving by glomerular basement membrane *in vitro*: effect of polycation or biochemical modifications. *Microvasc Res* 1991; 41: 311–327
33. Kanwar YS, Farquhar MG. Isolation of glycosaminoglycans (heparan sulfate) from glomerular basement membranes. *Proc Natl Acad Sci U S A* 1979; 76: 4493–4497
34. Nayak BR, Spiro RG. Localization and structure of the asparagine-linked oligosaccharides of type IV collagen from glomerular basement membrane and lens capsule. *J Biol Chem* 1991; 266: 13978–13987
35. Van Den Hoven MJ, Wijnhoven TJ, Li JP *et al*. Reduction of anionic sites in the glomerular basement membrane by heparanase does not lead to proteinuria. *Kidney Int* 2008; 73: 278–287
36. Chen S, Wassenhove-McCarthy DJ, Yamaguchi Y *et al*. Loss of heparan sulfate glycosaminoglycan assembly in podocytes does not lead to proteinuria. *Kidney Int* 2008; 74: 289–299
37. Dawes J, Pepper DS. Human vascular endothelial cells catabolise exogenous glycosaminoglycans by a novel route. *Thromb Haemost* 1992; 67: 468–472
38. Comper WD, Tay M, Wells X *et al*. Desulphation of dextran sulphate during kidney ultrafiltration. *Biochem J* 1994; 297(Pt 1): 31–34
39. Tay M, Comper WD, Singh AK. Charge selectivity in kidney ultrafiltration is associated with glomerular uptake of transport probes. *Am J Physiol* 1991; 260: F549–F554
40. Takeda T, McQuistan T, Orlando RA *et al*. Loss of glomerular foot processes is associated with uncoupling of podocalyxin from the actin cytoskeleton. *J Clin Invest* 2001; 108: 289–301

Received for publication: 27.10.08; Accepted in revised form: 17.12.08

Nephrol Dial Transplant (2009) 24: 2051–2058
doi: 10.1093/ndt/gfn757
Advance Access publication 22 January 2009

Indoxyl sulphate induces oxidative stress and the expression of osteoblast-specific proteins in vascular smooth muscle cells

Gulinuer Muteliefu[1], Atsushi Enomoto[2,3], Ping Jiang[3], Masahide Takahashi[3] and Toshimitsu Niwa[1]

[1]Department of Clinical Preventive Medicine, Nagoya University Hospital, [2]Institute for Advanced Research, Nagoya University and [3]Department of Pathology, Nagoya University Graduate School of Medicine, Nagoya, Japan

Correspondence and offprint requests to: Toshimitsu Niwa; E-mail: tniwa@med.nagoya-u.ac.jp

Abstract

Background. Previously, we demonstrated that indoxyl sulphate (IS), a uraemic toxin, induced aortic calcification in hypertensive rats. This study aimed to determine if IS induces the production of reactive oxygen species (ROS) and the expression of osteoblast-specific proteins in human aortic smooth muscle cells (HASMCs).

Methods. In order to achieve these goals, HASMCs were incubated with IS. ROS were detected using probes with a fluorescence detector. The expression of alkaline phosphatase (ALP), osteopontin and organic anion transporters (OAT1, OAT3) was studied by western blotting. The expression of core binding factor 1 (Cbfa1), ALP, osteopontin and NADPH oxidases (Nox1, Nox2 and Nox4) was analysed by reverse transcription-polymerase chain reaction (RT-PCR). Knockdown of Nox4 was performed by RNA interference (RNAi).

Results. IS induced ROS generation and the expression of Nox4, Cbfa1, ALP and osteopontin in HASMCs. A NADPH oxidase inhibitor and antioxidants inhibited IS-induced ROS production and mRNA expression of Cbfa1 and ALP. Knockdown of Nox4 using small interfering RNA (siRNA) inhibited IS-induced ROS production and mRNA expression of Cbfa1, ALP and osteopontin. OAT3 was expressed in HASMCs.

Conclusions. IS induces ROS generation by upregulating Nox4, and the expression of osteoblast-specific proteins such as Cbfa1, ALP and osteopontin in HASMCs.

Keywords: indoxyl sulphate; NADPH oxidase Nox4; osteoblast-specific proteins; reactive oxygen species; vascular smooth muscle cells

Introduction

Cardiovascular disease accounts for premature death in more than 50% of patients undergoing regular dialysis [1]. Cardiovascular disease mortality in dialysis patients is much higher especially in younger age categories than age- and sex-matched controls without chronic kidney disease (CKD) [1,2]. Vascular calcification plays a pivotal role in the development of cardiovascular morbidity and subsequent increased mortality. Vascular calcification affects both vascular intima and media layers, and its mechanism remains poorly understood. In addition to traditional cardiovascular risk factors, hyperphosphataemia, calcium overload, increased oxidized low-density lipoprotein cholesterol, uraemic toxins, increased oxidative stress, hyperhomocysteinaemia, haemodynamic overload and

© The Author [2009]. Published by Oxford University Press on behalf of ERA-EDTA. All rights reserved.
For Permissions, please e-mail: journals.permissions@oxfordjournals.org

Downloaded from https://academic.oup.com/ndt/article/24/7/2051/1910764 by guest on 21 August 2022

dialysate-related factors may also play a role in vascular calcification [3].

High levels of inorganic phosphate and uraemic serum can transform vascular smooth muscle cells (VSMCs) into osteoblast-like cells, possibly by upregulating the expression of core binding factor 1 (Cbfa1/Runx2) [4–8]. Addition of β-glycerophosphate as a donor of inorganic phosphate induced calcification and osteopontin expression in cultured VSMCs [5]. Addition of uraemic serum also accelerated mineralization and increased expression of Cbfa1, osteopontin and alkaline phosphatase (ALP) in cultured VSMCs [4–8]. Besides inorganic phosphate, unknown uraemic toxins are considered to be responsible for the osteoblastic transformation of VSMCs.

Indoxyl sulphate (IS) is a uraemic toxin that accelerates the progression of CKD [9,10], and is derived from dietary protein. A part of protein-derived tryptophan is metabolized into indole by tryptophanase of intestinal bacteria such as *Escherichia coli*. Indole is absorbed into the blood from the intestine, and is metabolized in the liver to IS, which is normally excreted into urine. In CKD, however, a decrease in renal clearance of IS leads to its increased serum levels [11–13]. Administration of IS and its precursor, indole, to five of six nephrectomized rats stimulated glomerular sclerosis in the remnant kidney accompanied by a decline in renal function [12,14]. Further, IS stimulated transcription of genes related to renal fibrosis, such as transforming growth factor (TGF) β1, tissue inhibitor of metalloproteinases (TIMP) 1 and pro-α1 collagen [15,16]. The induction of nephrotoxicity by IS is mediated by organic anion transporters (OATs), such as OAT1 and OAT3, which are localized in the basolateral membrane of renal proximal tubular cells [17]. IS reduced superoxide scavenging activity in the kidneys of normal and uraemic rats [18]. Thus, the nephrotoxicity of IS may be induced by stimulating the production of reactive oxygen species (ROS) and impairing the anti-oxidative system in the kidney.

IS inhibits endothelial proliferation and wound repair [19], and induces oxidative stress in endothelial cells [20]. IS stimulates proliferation of rat VSMCs [21]. These *in vitro* experiments suggest that IS may play a role in the dysfunction of endothelial and vascular smooth muscle cells in CKD patients. Recently, we have demonstrated that IS promoted aortic calcification with expression of osteoblast-specific proteins such as Cbfa1, ALP, and osteopontin, in hypertensive rats [22]. We hypothesized that accumulation of IS in CKD stage 5 may stimulate osteoblastic differentiation of VSMCs, followed by aortic calcification.

This study aimed to determine if IS induces the production of ROS and the expression of osteoblast-specific proteins such as Cbfa1, ALP and osteopontin in human aortic smooth muscle cells (HASMCs). The present study demonstrated that IS stimulated the production of ROS by upregulating NADPH oxidase Nox4, and induced the expression of the osteoblast-specific proteins in HASMCs.

Methods

Reagents

Indoxyl sulphate (IS), diphenylene iodonum chloride (DPI), rotenone, 2-thenoyltrifluoroacetone (TTFA), allopurinol, oxypurinol, *N*-nitro-L-arginine methyl ester (L-NAME), *N*-acetylcysteine (NAC), vitamin C, vitamin E and Dulbecco's phosphate buffered saline (D-PBS) were purchased from Sigma-Aldrich (St Louis, MO, USA). Human serum albumin (HSA) for intravenous use was purchased from Mitsubishi Tanabe Pharma Co. (Osaka, Japan). Apocynin was purchased from Calbiochem (CBC, Darmstadt, Germany). HASMCs were purchased from Cascade Biologics (Portland, OR, USA). Dulbecco's modified Eagle's medium (D-MEM), Hanks' balanced salt solution (HBSS), OPTI-MEM I reduced serum medium, fetal bovine serum (FBS), penicillin–streptomycin and trypsin–EDTA solution were purchased from Gibco (Invitrogen, Grand Island, NY, USA). The 5- (and -6) chloromethyl-2′,7′-dichlorodihydrofluorescein diacetate acetyl ester (CM-H_2DCFDA) and dihydroethidium (DHE) were purchased from Molecular Probes (Eugene, OR, USA). ECL Western Blotting detection reagents were purchased from GE Healthcare (Amersham, UK). BCA Protein Assay Kit was purchased from Pierce (Rockford, IL, USA). High Pure RNA Isolation Kit, 1st Strand cDNA Synthesis Kit for reverse transcription-polymerase chain reaction (RT-PCR) (AMV) and LightCycler FastStart DNA Master SYBR Green I were purchased from Roche Diagnostics (Mannheim, Germany). LightCycler-Primer Set of human glyceraldehyde-3-phosphate dehydrogenase (GAPDH), human Cbfa1, human ALP and human osteopontin were purchased from Search-LC (Heidelberg, Germany). Human Nox1, Nox2 and Nox4 primers were purchased from Nihon Gene Research Laboratories (Sendai, Japan). Antibodies used in this study include mouse monoclonal anti-human osteopontin antibody (ARP, Belmont, MA, USA), mouse monoclonal anti-human ALP antibody (R&D Systems, Minneapolis, MN, USA), rabbit polyclonal anti-human OAT3 and OAT1 antibodies (Trans Genic, Kumamoto, Japan), mouse monoclonal anti-human β-actin antibody (Sigma-Aldrich, St Louis, MO, USA), horseradish peroxidase-conjugated rabbit anti-mouse IgG antibody, and swine anti-rabbit IgG antibody (Dako Cytomation, Glostrup, Denmark). Lipofectamine 2000 was purchased from Invitrogen (Carlsbad, CA, USA). Human Nox4 siRNA and control siRNA were purchased from Qiagen (Valencia, CA, USA). AmpliTaq Gold Taq DNA polymerase was purchased from Applied Biosystems (Foster City, CA, USA).

Cell culture

HASMCs were maintained in D-MEM containing 10% FBS supplemented with 100 U/ml penicillin and 100 μg/ml streptomycin at 37°C under 5% CO_2 humidified atmosphere. The medium was replaced every 2 days until confluence. Only cells between passages 2 and 5 were used for experiments.

Measurement of ROS production

To investigate the effects of IS on the generation of ROS in HASMCs, the fluorescence intensity of CM-H_2DCFDA used as a ROS probe was measured. HASMCs(10^4 cells/well) were preincubated with the culture medium in 96-well plates at 37°C for 24 h. Confluent HASMCs were then loaded with 10 μM CM-H_2DCFDA in D-PBS at 37°C for 30 min. After removing the medium from wells, cells were treated with different concentrations of IS (100, 250, 500, 1000 μM) for 3 h, in the presence or absence of 4% HSA. Control experiments were done without IS in parallel with the ones testing IS.

To determine the time course of IS-induced ROS production in HASMCs, cells were treated with 500 μM IS at 37°C for 0.5–3 h. Control experiments were done without IS at 0 time.

HASMCs were incubated with IS (500 μM) for 3 h in the presence of an inhibitor of NADPH oxidase (10 μM DPI), 50 μM apocynin, inhibitors of xanthine oxidase (100 μM oxypurinol and 100 μM allopurinol), an inhibitor of NO synthase (1 mM L-NAME) and inhibitors of mitochondrial electron transport (10 μM rotenone, 10 μM TTFA), or in the presence of antioxidants, NAC (5 mM), vitamin E (10 μg/ml) and vitamin C (200 μM). The fluorescence intensity was measured at 485 nm for excitation and 527 nm for emission using a fluorescence microplate reader. The mean fluorescence intensity ratio is presented as the percentage of the control value, after subtraction of background fluorescence. Control experiments were done without IS in parallel with the ones testing the various samples. The fluorescence intensity of IS in distilled water at 485 nm for excitation and 527 nm for emission was negligible.

Superoxide anion was detected using the fluoroprobe DHE. HASMCs (10^4 cells/well) were pre-incubated with culture medium in 96-well plates at 37°C for 24 h, and treated with different concentrations of IS (100, 250, 500, 1000 μM) for 3 h; then cells were stained with 10 μM DHE dissolved

Downloaded from https://academic.oup.com/ndt/article/24/7/2051/1910764 by guest on 21 August 2022

in HBSS containing $CaCl_2$ and $MgCl_2$ at 37°C for 45 min. After staining, cells were washed with HBSS to remove excess dyes, and fluorescence was monitored at 485 nm for exitation and 595 nm for emission using a fluorescence microplate reader. The mean fluorescence intensity ratio is presented as the percentage of the control value, after subtraction of background fluorescence. Control experiments were done without IS in parallel with the ones testing IS.

Western blot analysis

HASMCs cultured in 60-mm dishes were stimulated by IS at different concentrations for 48 h. Control cultures were used without IS. Cells were lysed in a lysis buffer [1% Triton X, 20 mM Tris–HCl (pH 7.4), 150 mM NaCl, 1 mM EDTA and 0.5 mM sodium orthovandate). Proteins were quantified by using BCA Protein Assay Kit, separated by 10% SDS–polyacrylamide gel electrophoresis (SDS–PAGE), and electrophoretically transferred to nitrocellulose membranes. The membranes were blocked with 4% skim milk in PBS for 1 h at room temperature, and then incubated with mouse monoclonal anti-human ALP antibody (1:200), mouse monoclonal anti-human osteopontin antibody (1:1000), rabbit polyclonal anti-human OAT3 and OAT1 antibodies (1:100 and 1:200, respectively) and mouse monoclonal anti-human β-actin antibody (1:1000) overnight at 4°C. The membrane was washed with 0.05% Tween-20 (T-PBS), and then the horseradish peroxidase-conjugated rabbit anti-mouse IgG antibody (1:1000) and swine anti-rabbit IgG antibody (1:1000) were used for the detection of the target proteins. The immunodetection was accomplished using the ECL western blotting detection reagents. The band intensity was analysed by scanning densitometry. The protein levels were normalized with β-actin, an internal control.

Total RNA isolation and quantitative RT-PCR analysis

HASMCs cultured in 60-mm dishes were stimulated by IS at different concentrations for 24 h. Total RNA was extracted from the cultured cells using High Pure RNA Isolation Kit. The purity and quantity of the RNA preparation were determined by measuring the optical densities at 260 and 280 nm.

To estimate the mRNA levels of Cbfa1 and ALP, quantitative RT-PCR was performed using the LightCycler system (Roche Diagnostics). Total RNA was reversely transcribed with random hexamers using 1st Strand cDNA Synthesis Kit for RT-PCR (AMV). The reaction was processed as follows: incubation of samples at 25°C for 10 min and then at 42°C for 60 min, followed by 99°C for 5 min and cooling to 4°C for 5 min. The quantitative PCR was performed with the LightCycler instrument using LightCycler FastStart DNA Master SYBR Green I, LightCycler-Primer Set, human Nox1 primer (forward: 5′TGGATCACAACCTCACCT3′; reverse: 5′ACTGGATGGGATTTAG CC3′), human Nox2 primer (forward: 5′CCAGTGAAGATGTGTTCA GCT3′; reverse: 5′GCACAGCCAGTAGAAGTAGAT3′) and Nox4 primer (forward: 5′AGTCAAACAGATGGGATA3′; reverse: 5′TGTCCCATA TGAGTTGTT3′). The LightCycler system consists of a rapid PCR cycler and fluorescence-detection component, which allows real-time monitoring of fluorescence during PCR amplification. SYBR Green I, a double-strand DNA-binding fluorescent dye, was chosen to monitor cDNA amplication. The expression of mRNA levels is measured as the ratio of each mRNA and the GAPDH mRNA.

RNA interference for knockdown of human Nox4

RNA interference (RNAi)-mediated knockdown of human Nox4 was performed according to the method by Elbashir *et al*. [23]. HASMCs were transfected with Nox4 siRNA or a 21-nucleotide control siRNA using Lipofectamine 2000 and OPTI-MEM I according to the manufacture's protocol. Thirty to fifty percent confluent HASMCs were incubated in the serum-free medium without antibiotics for several hours before transfection. The transfection medium was prepared by mixing 200 pmol siRNA oligomer and 5 μl lipofectamine 2000 in 500 μl OPTI-MEM I, respectively, incubated at room temperature for 5 min. The mixtures were combined and incubated at room temperature for further 20 min. Cells were incubated with the transfection medium for 6 h in the incubator before changing back to the normal medium. Forty-eight hours after the transfection, the cells were used for the experiments.

Polymerase chain reaction

PCR was performed using human Nox4 and GAPDH-specific primers by AmpliTaq Gold Taq DNA polymerase according to the instruction of the manufacturer. PCR products were electrophoresed on a 2% agarose gel for 20 min at 100 V, and bands were visualized by an ultraviolet transilluminator using FAS-III (Toyobo, Tokyo, Japan) after staining with ethidium bromide.

Statistical analysis

Results are expressed as mean ± SE. To compare values among the groups of three or more, analysis of variance (ANOVA) and Fisher's protected least-significance difference (PLSD) test were performed. Results were considered statistically significant when P-value was < 0.05.

Results

Effects of IS on ROS generation in HASMCs

To clarify whether IS induces oxidative stress in HASMCs, the effect of IS on ROS production by HASMCs was determined. IS increased ROS production by HASMCs in a time-dependent manner reaching a maximum after 3 h (Figure 1A). IS significantly increased ROS production by HASMCs in a concentration-dependent manner (Figure 1B). Because IS is mainly bound to albumin in blood, the effects of IS on ROS production in HASMCs were determined in the presence of 4% HSA in the medium. IS, even in the presence of 4% HSA, increased ROS production in HASMCs (Figure 1C).

An additional probe was used to detect ROS. Superoxide anion was detected using the fluoroprobe DHE. IS significantly increased superoxide production by HASMCs in a concentration-dependent manner (Figure 1D).

To study the mechanism of IS-mediated ROS production, the role of pro-oxidative enzymes such as NADPH oxidase and xanthione oxidase, and of mitochondrial electron transport was investigated. ROS production by HASMCs was measured after treatment with IS in the presence of an inhibitor of NADPH oxidase (DPI), apocynin, inhibitors of xanthine oxidase (oxypurinol, allopurinol), and inhibitors of mitochondrial electron transport (rotenone, TTFA). The IS-induced ROS production was significantly inhibited by DPI and apocynin (Figure 2A). Apocynin was considered to be an inhibitor of NADPH oxidase, but has been demonstrated to be not an inhibitor of NADPH oxidase but an antioxidant in vascular smooth muscle cells and endothelial cells [24]. The other inhibitors, however, showed no significant effects on IS-induced ROS production. Thus, IS-induced ROS production by HASMCs is mediated most likely by activation of NADPH oxidase.

To study the involvement of NO synthase, ROS production was examined in the presence of L-NAME, an inhibitor of NO synthase. L-NAME did not affect the IS-induced ROS production by HASMCs (Figure 2A).

The addition of antioxidants such as vitamin C, vitamin E and NAC significantly inhibited the IS-induced ROS production by HASMCs (Figure 2B). The addition of vitamin C and NAC reduced ROS levels lower than control, whereas vitamin E reduced ROS to almost control levels. Both vitamin C and NAC, even in the absence of IS, significantly reduced ROS generation by HASMCs.

Downloaded from https://academic.oup.com/ndt/article/24/7/2051/1910764 by guest on 21 August 2022

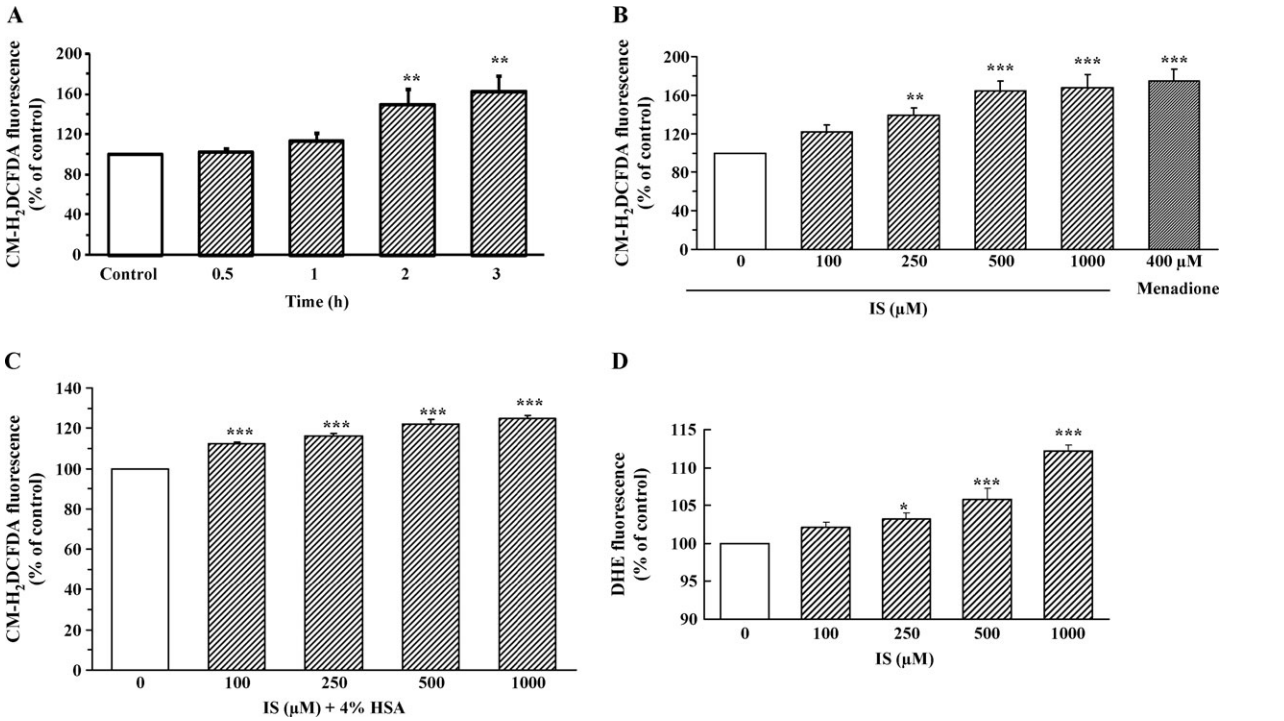

Fig. 1. (**A**) Time course of IS-induced ROS production in HASMCs. (**B**) Effect of IS on ROS production in HASMCs. Menadione was used as a positive control. (**C**) Effect of IS on ROS production in HASMCs in the presence of 4% human serum albumin (HSA). (**D**) Effect of IS on superoxide generation in HASMCs. Results are expressed as percents in the fluorescence intensity compared to control (0 μM IS) (mean ± SE, $n = 15$, $^{*}P < 0.05$, $^{**}P < 0.01$, $^{***}P < 0.001$ versus control).

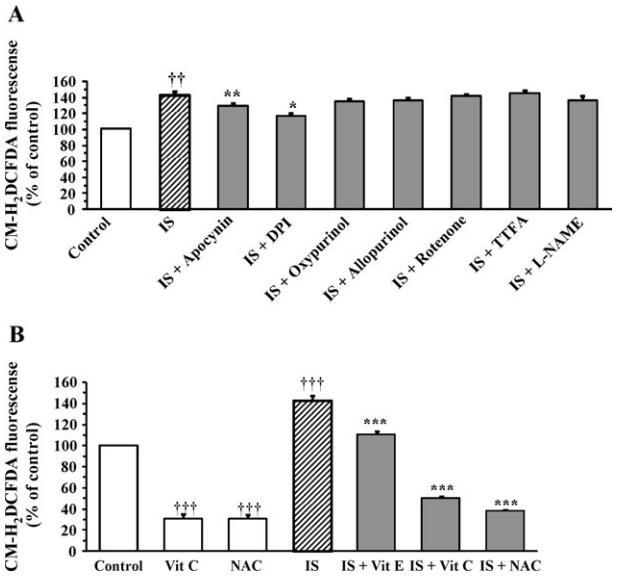

Fig. 2. Effect of inhibitors and antioxidants on IS-induced ROS production in HASMCs. (**A**) Effect of inhibitors of pro-oxidative enzymes on IS-induced ROS production in HASMCs. (**B**) Effect of antioxidants on IS-induced ROS production in HASMCs. Results are expressed as percents in the fluorescence intensity compared to control (mean ± SE, $n = 15$, $^{\dagger\dagger}P < 0.01$ versus control, $^{\dagger\dagger\dagger}P < 0.001$ versus control, $^{*}P < 0.05$, $^{**}P < 0.01$, $^{***}P < 0.001$ versus IS).

Effects of IS on expression of osteoblast-specific proteins in HASMCs

ALP is a phenotypic marker of osteoblasts and is essential for vascular calcification. The effect of IS on ALP expression was studied by incubating HASMCs with 500 μM IS for 48 h. Western blot analysis demonstrated that the addition of IS at 500 μM significantly increased ALP expression in HASMCs (Figure 3A and B).

Osteopontin is a marker protein of osteoblast transformation. The effect of IS on osteopontin expression was studied by incubating HASMCs with IS at concentrations ranging from 100 to 500 μM for 48 h. Western blot analysis demonstrated that IS stimulated the expression of osteopontin in HASMCs in a concentration-dependent manner (Figure 3C and D).

IS is transported by OAT1 and OAT3 in the basolateral membranes of renal tubular cells. In the present study, HASMCs were incubated with IS at different concentrations from 100 to 500 μM for 48 h. Protein expression of OAT1 and OAT3 was determined by western blotting. Expression of OAT3 was observed in HASMCs (Figure 3E), whereas expression of OAT1 was hardly detected in HASMCs (data not shown). There were no changes in the expression of OAT3 in HASMCs regardless of the presence of IS at different concentrations.

RT-PCR demonstrated that IS significantly increased the mRNA expression of Cbfa1, ALP, and osteopontin mRNA in HASMCs in a concentration-dependent manner (data not shown). The increase in the IS-induced mRNA expression of Cbfa1 was significantly inhibited by the addition of DPI, an inhibitor of NADPH oxidase, and antioxidants such as vitamin E, vitamin C and NAC (Figure 4A). The increase in the IS-induced mRNA expression of ALP was also significantly inhibited by the addition of DPI, vitamin C and NAC (Figure 4B).

Downloaded from https://academic.oup.com/ndt/article/24/7/2051/1910764 by guest on 21 August 2022

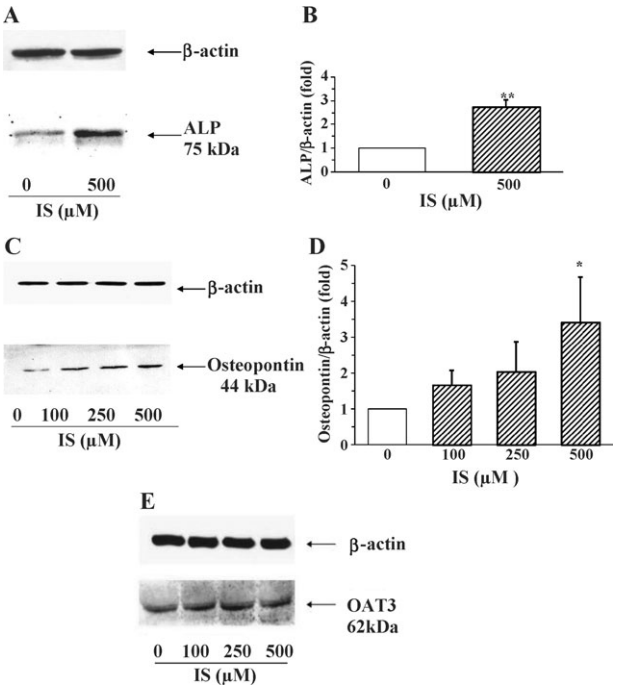

Fig. 3. Effect of IS on protein expression of ALP, osteopontin and OAT3 in HASMCs. (**A**) Representative immunoblots with anti-ALP and anti-β-actin antibodies after stimulation with 500 μM IS. (**B**) Densitometric analysis of ALP normalized by β-actin. (**C**) Representative immunoblots with anti-osteopontin and anti-β-actin antibodies after stimulation with different concentrations of IS. (**D**) Densitometric analysis of osteopontin normalized by β-actin. (**E**) Representative immunoblots with anti-OAT3 and anti-β-actin antibodies after stimulation with different concentrations of IS. The results are shown as the fold in expression as compared to control (0 μM IS) (mean ± SE, $n = 3$, $^{*}P < 0.05$, $^{**}P < 0.01$ versus 0 μM IS).

Effects of IS on the expression of the subunits of NADPH oxidase in HASMCs

We determined by using RT–PCR if IS induces the expression of Nox1, Nox2 and Nox4 mRNA in HASMCs. IS significantly increased Nox4 mRNA expression in HASMCs at concentrations of 250 μM and 500 μM (Figure 5), whereas it did not significantly increase the mRNA expression of Nox1 or Nox2 (data not shown).

Effects of Nox4 knockdown on IS-induced ROS production and mRNA expression of osteoblast-specific proteins in HASMCs

To further study the role of Nox4 in the mechanism of IS-mediated ROS production, we specifically knocked down Nox4 in HASMCs using the RNAi method. Transfection of HASMCs with siRNA specific to human Nox4 led to a significant decrease in the mRNA for Nox4, as estimated by RT–PCR (Figure 6A). IS-induced ROS production was inhibited by Nox4 siRNA in HASMCs (Figure 6B). The upregulation of Cbfa1, ALP and osteopontin mRNA expression induced by IS was prevented by Nox4 siRNA in HASMCs (Figure 6C–E). Thus, Nox4 is involved in IS-induced ROS production and expression of osteoblast-specific proteins in HASMCs.

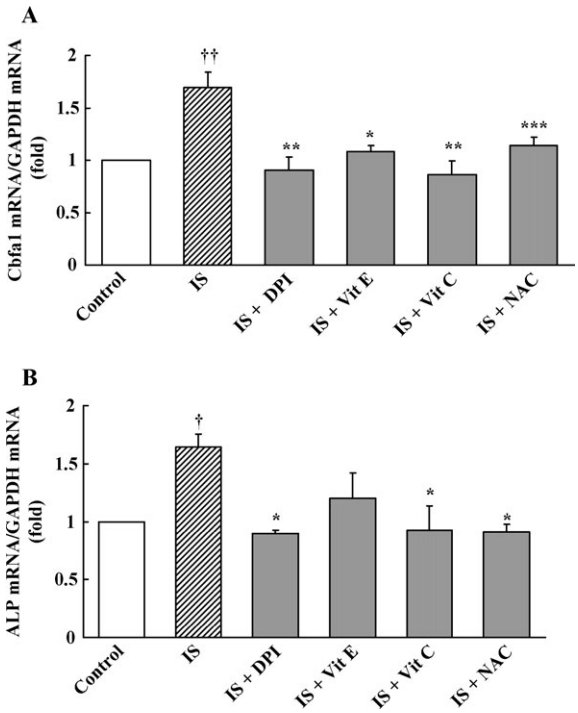

Fig. 4. Effects of an NADPH oxidase inhibitor and antioxidants on IS-induced mRNA expression of Cbfa1 and ALP in HASMCs. Expression of mRNA level for (**A**) Cbfa1 and (**B**) ALP was normalized to GAPDH. The results are shown as the fold in expression as compare to control (mean ± SE, $n = 3$, $^{\dagger}P < 0.05$, $^{\dagger\dagger}P < 0.01$ versus control, $^{*}P < 0.05$, $^{**}P < 0.01$, $^{***}P < 0.001$ versus IS).

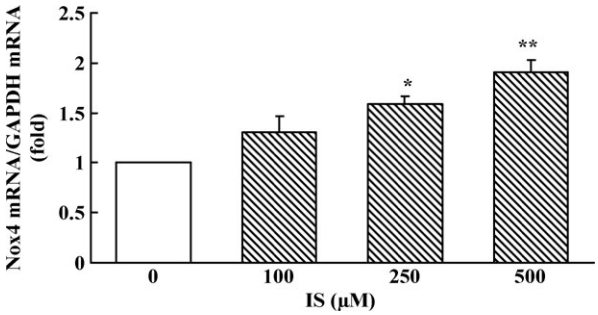

Fig. 5. Effects of IS on mRNA expression of NADPH oxidase Nox4 in HASMCs. Expression of mRNA levels for Nox4 was normalized to GAPDH. The results are shown as the fold in expression as compared to control (0 μM IS) (mean ± SE, $n = 4$, $^{*}P < 0.05$, $^{**}P < 0.01$ versus 0 μM IS).

Discussion

Herein, we show for the first time that IS stimulated ROS generation by upregulating NADPH oxidase Nox4, and induced the expression of osteoblast-specific proteins such as Cbfa1, ALP and osteopontin in HASMCs. These effects of IS were observed even at a concentration of IS found in haemodialysis patients, because the mean serum level of IS in haemodialysis patients was 249 μM [12] or 360 μM [13] and the maximum serum level of IS was 557 μM.

Our results show that ROS derived from NADPH oxidase Nox4 are important for the induction of

Downloaded from https://academic.oup.com/ndt/article/24/7/2051/1910764 by guest on 21 August 2022

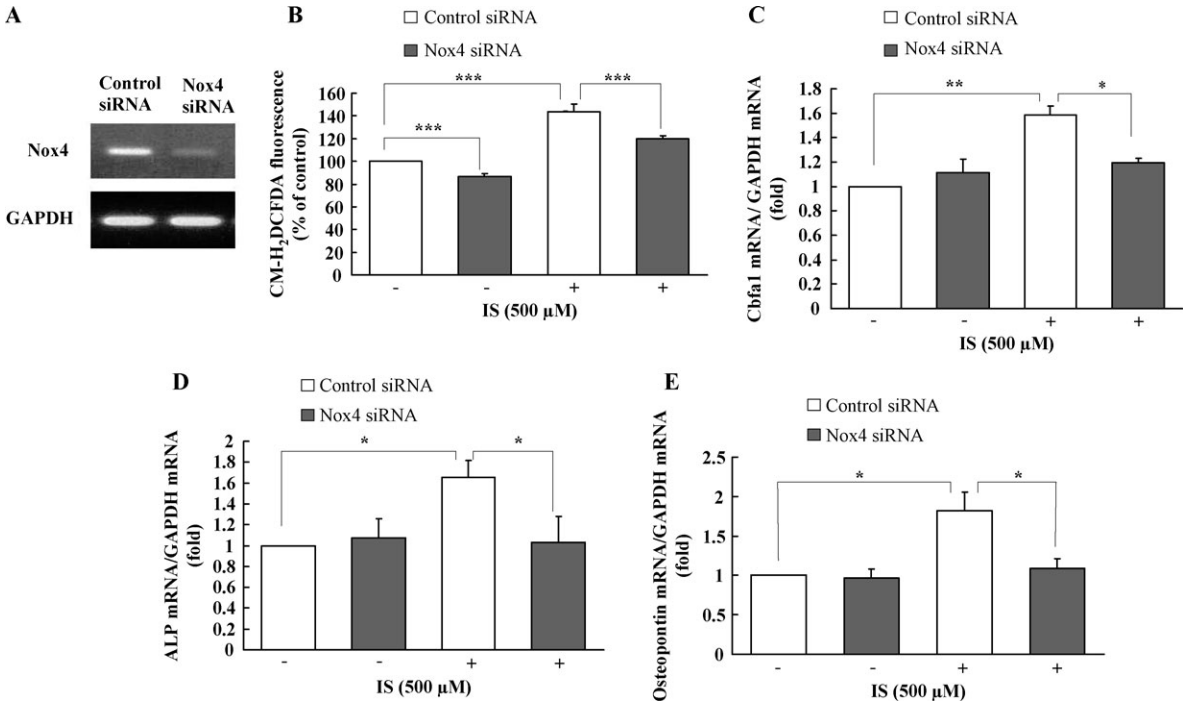

Fig. 6. Effect of Nox4 siRNA on IS-induced ROS production and mRNA expression of osteoblast-specific proteins in HASMCs. (**A**) Representative gels for Nox4 and GAPDH gene expression. (**B**) Effect of Nox4 siRNA on IS-induced ROS production in HASMCs (mean ± SE, $n = 8$, $^{***}P < 0.001$). Effects of Nox4 siRNA on IS-induced mRNA expression for (**C**) Cbfa1, (**D**) ALP and (**E**) osteopontin normalized to GAPDH (mean ± SE, $n = 4$, $^{*}P < 0.05$, $^{**}P < 0.01$).

transdifferentiation of HASMCs into cells with a more osteoblastic phenotype. Inhibition by DPI is suggestive evidence to implicate NADPH oxidases in a response. NADPH oxidase enzyme complex produces superoxide anion in conjunction with oxidation of NAD(P)H. The Nox family of NADPH oxidase comprises five members (Nox1 to Nox5) and the Duox family two (Duox1 and Duox2) [25]. Nox1, Nox2 and Nox4 are present in VSMCs [26–28]. Lassègue *et al*. found that both Nox1 and Nox4 are expressed to a much higher degree than Nox2 in VSMCs [27]. Both generate ROS in VSMCs but differ in their response to growth factors. Nox1 is co-localized with caveolin in punctate patches on the surface and along the cellular margins, whereas Nox4 is co-localized with vinculin in focal adhesions [28]. To identify a particular Nox in IS-induced responses, we analysed the mRNA expression of Nox1, Nox2 and Nox4 in HASMCs incubated with IS, and found that IS significantly increased the mRNA expression of Nox4 but not significantly Nox1 or Nox2. Further, knockdown of Nox4 by siRNA was performed to determine if Nox4 mediates the response of Cbfa1, ALP and osteopontin to IS. We demonstrated that the knockdown of Nox4 inhibited the IS-induced mRNA expression of the Cbfa1, ALP and osteopontin as well as ROS production.

Previous studies showed that IS enhanced ROS production and induced cellular toxicity in endothelial cells [19], glomerular mesangial cells [29], renal tubular cells [30] and osteoblasts [31]. Dou *et al*. [19] found that IS increased NADPH oxidase activity and decreased glutathione levels in endothelial cells. Gelasco *et al*. [29] found that IS induced the production of intracellular ROS in mesangial cells, and the ROS generation was partially inhibited by an inhibitor of NADPH oxidase. Motojima *et al*. [30] found that IS induced free radical production in renal tubular cells, and activated NF-kappaB which, in turn, upregulated PAI-1 expression. Nii-Kono *et al*. [31] found that IS enhanced oxidative stress in osteoblasts to impair osteoblast function and down-regulated PTHR expression.

OAT1 and OAT3 are expressed in the basolateral membranes of proximal tubular cells in the kidney, and up-take IS from blood into tubular cells [17]. Recently, OAT3 was identified in the primary osteoblast culture, and IS taken up by osteoblasts via OAT3 enhanced oxidative stress [31]. In the present study, we showed that OAT3 is expressed in HASMCs. This finding suggests that OAT3 is involved in the transport of IS into VSMCs. Then, IS induces the production of ROS in VSMCs by upregulating the expression of Nox4, and consequently promotes the expression of osteoblast-specific proteins such as Cbfa1, ALP and osteopontin.

Although the pathogenesis of vascular calcification in uraemia is not yet completely understood, uraemic vascular calcification is an active, cell-mediated process resembling osteogenesis in bone rather than passive precipitation. Moe *et al*. [4–8] identified increased expression of bone-associated proteins (osteopontin, ALP, bone sialoprotein, type I collagen) and the bone-specific transcription factor Cbfa1 in histologic sections of inferior epigastric arteries obtained from patients with stage 5 CKD or calcific uraemic arteriolopathy. The addition of

Downloaded from https://academic.oup.com/ndt/article/24/7/2051/1910764 by guest on 21 August 2022

uraemic serum to cultured VSMCs upregulated osteopontin and Cbfa1 expression and accelerated mineralization [4–8]. The uraemic serum-induced osteopontin expression in VSMCs is partially mediated through ALP activity and type III sodium-dependent phosphate co-transporter (Pit-1)-dependent mechanism. Thus, uraemic milieu may lead to differentiation of VSMCs, with subsequent mineralization.

VSMCs and osteoblasts are derived from mesenchymal precursor cells. Cbfa1 is a pivotal transcriptional regulator of osteogenesis, and is used as a molecular marker to detect the transdifferentiation of VSMCs to osteoblastic phenotype. By binding to and regulating the expression of specific genes, Cbfa1 plays a key role in the differentiation of mesenchymal cells to osteoblasts. ALP is considered a phenotypic marker of osteoblasts that is critical for bone mineralization. Osteopontin is an acidic phosphoprotein normally found in bone, teeth, kidneys and epithelial lining tissues. Osteopontin is secreted to the mineralizing extracellular matrix by osteoblasts during the bone development, facilitating the attachment of osteoblasts to the extracellular matrix. The upregulation of osteopontin is associated with vascular calcification. Hyperphosphataemia or azotaemia was associated with the expression of osteopontin in VSMCs in patients with stage 5 CKD [32]. Thus, accumulation of inorganic phosphate and/or uraemic toxins plays an important role in osteoblastic differentiation of VSMCs.

Recently, we demonstrated that IS promoted aortic calcification in hypertensive rats, and that osteoblast-specific proteins such as Cbfa1, ALP and osteopontin were colocalized in the cells embedded in the aortic calcification area [22]. In the present study, IS induced oxidative stress by upregulating NADPH oxidase Nox4, and the expression of osteoblast-specific proteins such as Cbfa1, ALP and osteopontin in VSMCs. Taken together, accumulation of IS in blood due to renal dysfunction may be one of the risk factors for the development of aortic calcification in CKD patients.

Acknowledgement. I acknowledge Aichi Kidney Foundation for funding our study.

Conflict of interest statement. None declared.

References

1. Foley RN, Parfrey PS, Sarnak MJ. Clinical epidemiology of cardiovascular disease in chronic renal disease. *Am J Kidney Dis* 1998; 32: S112–S119
2. Johnson DW, Craven AM, Isbel NM. Modification of cardiovascular risk in hemodialysis patients: an evidence-based review. *Hemodial Int* 2007; 11: 1–14
3. Derici U, El Nahas AM. Vascular calcifications in uremia: old concepts and new insights. *Semin Dial* 2006; 19: 60–68
4. Moe SM, O'Neill KD, Duan D *et al*. Medial artery calcification in ESRD patients is associated with deposition of bone matrix proteins. *Kidney Int* 2002; 61: 638–647
5. Chen NX, O'Neill KD, Duan D *et al*. Phosphorus and uremic serum up-regulate osteopontin expression in vascular smooth muscle cells. *Kidney Int* 2002; 62: 1724–1731
6. Moe SM, Duan D, Doehle BP *et al*. Uremia induces the osteoblast differentiation factor Cbfa1 in human blood vessels. *Kidney Int* 2003; 63: 1003–1011
7. Chen NX, Moe SM. Vascular calcification in chronic kidney disease. *Semin Nephrol* 2004; 24: 61–68
8. Chen NX, Duan D, O'Neill KD *et al*. The mechanisms of uremic serum-induced expression of bone matrix proteins in bovine vascular smooth muscle cells. *Kidney Int* 2006; 70: 1046–1053
9. Niwa T. Uremic Toxicity, Indoxyl sulfate. In: Massry SG, Glassock RJ (eds). *Textbook of Nephrology*. Philadelphia, PA: Lippincott Williams & Wilkins, 2001, 1269–1272.
10. Niwa T. Organic acids and the uremic syndrome: protein metabolite hypothesis in the progression of chronic renal failure. *Semin Nephrol* 1996; 16: 167–182
11. Niwa T, Takeda N, Tatematsu A *et al*. Accumulation of indoxyl sulfate, an inhibitor of drug-binding, in uremic serum as demonstrated by internal-surface reversed-phase liquid chromatography. *Clin Chem* 1988; 34: 2264–2267
12. Niwa T, Ise M. Indoxyl sulfate, a circulating uremic toxin, stimulates the progression of glomerular sclerosis. *J Lab Clin Med* 1994; 124: 96–104
13. Niwa T, Miyazaki T, Tsukushi S *et al*. Accumulation of indoxyl-β-D-glucuronide in uremic serum: suppression of its production by oral sorbent and efficient removal by hemodialysis. *Nephron* 1996; 74: 72–78
14. Niwa T, Ise M, Miyazaki T. Progression of glomerular sclerosis in experimental uremic rats by administration of indole, a precursor of indoxyl sulfate. *Am J Nephrol* 1994; 14: 207–212
15. Miyazaki T, Ise M, Seo H *et al*. Indoxyl sulfate increases the gene expressions of TGF-β_1, TIMP-1 and pro α(I) collagen in uremic rat kidneys. *Kidney Int* 1997; 52(S62): S15–S22
16. Miyazaki T, Ise M, Hirata M *et al*. Indoxyl sulfate stimulates renal synthesis of transforming growth factor-β_1 and progression of renal failure. *Kidney Int* 1997; 52(Suppl 63): S211–S214
17. Enomoto A, Takeda M, Tojo A *et al*. Role of organic anion transporters in the tubular transport of indoxyl sulfate and the induction of its nephrotoxicity. *J Am Soc Nephrol* 2002; 13: 1711–1720
18. Owada S, Goto S, Bannai K *et al*. Indoxyl sulfate reduces superoxide scavenging activity in the kidneys of normal and uremic rats. *Am J Nephrol* 2008; 28: 446–454
19. Dou L, Bertrand E, Cerini C *et al*. The uremic solutes *p*-cresol and indoxyl sulfate inhibit endothelial proliferation and wound repair. *Kidney Int* 2004; 65: 442–451
20. Dou L, Jourde-Chiche N, Faure V *et al*. The uremic solute indoxyl sulfate induces oxidative stress in endothelial cells. *J Thromb Haemost* 2007; 5: 1302–1308
21. Yamamoto H, Tsuruoka S, Ioka T *et al*. Indoxyl sulfate stimulates proliferation of rat vascular smooth muscle cells. *Kidney Int* 2006; 69: 1780–1785
22. Adijiang A, Goto S, Uramoto S *et al*. Indoxyl sulphate promotes aortic calcification with expression of osteoblast-specific proteins in hypertensive rats. *Nephrol Dial Transplant* 2008; 23: 1892–1901
23. Elbashir SM, Harborth J, Lendeckel W *et al*. Duplexes of 21-nucleotide RNAs mediate RNA interference in cultured mammalian cells. *Nature* 2001; 411: 494–498
24. Heumüller S, Wind S, Barbosa-Sicard E *et al*. Apocynin is not an inhibitor of vascular NADPH oxidases but an antioxidant. *Hypertension* 2008; 51: 211–217
25. Geiszt M. NADPH oxidases: new kids on the block. *Cardiovasc Res* 2006; 71: 289–299
26. Suh YA, Arnold RS, Lassegue B *et al*. Cell transformation by the superoxide-generating oxidase Mox1. *Nature* 1999; 401: 79–82
27. Lassègue B, Sorescu D, Szöcs K *et al*. Novel gp91(phox) homologues in vascular smooth muscle cells: nox1 mediates angiotensin II-induced superoxide formation and redox-sensitive signaling pathways. *Circ Res* 2001; 88: 888–894

Downloaded from https://academic.oup.com/ndt/article/24/7/2051/1910764 by guest on 21 August 2022

28. Hilenski LL, Clempus RE, Quinn MT *et al*. Distinct subcellular localizations of Nox1 and Nox4 in vascular smooth muscle cells. *Arterioscler Thromb Vasc Biol* 2004; 24: 677–683
29. Gelasco AK, Raymond JR. Indoxyl sulfate induces complex redox alterations in mesangial cells. *Am J Physiol Renal Physiol* 2006; 290: F1551–F1558
30. Motojima M, Hosokawa A, Yamato H *et al*. Uremic toxins of organic anions up-regulate PAI-1 expression by induction of NF-kappaB and free radical in proximal tubular cells. *Kidney Int* 2003; 63: 1671–1680
31. Nii-Kono T, Iwasaki Y, Uchida M *et al*. Indoxyl sulfate induces skeletal resistance to parathyroid hormone in cultured osteoblastic cells. *Kidney Int* 2007; 71: 738–743
32. Nakamura H, Honda H, Inada Y *et al*. Osteopontin expression in vascular smooth muscle cells in patients with end-stage renal disease. *Ther Apher Dial* 2006; 10: 273–277

Received for publication: 21.8.08; Accepted in revised form: 17.12.08

Nephrol Dial Transplant (2009) 24: 2058–2067
doi: 10.1093/ndt/gfn752
Advance Access publication 20 January 2009

Downloaded from https://academic.oup.com/ndt/article/24/7/2051/1910764 by guest on 21 August 2022

Regulation of amino acid transporters in the rat remnant kidney

João S. Amaral, Maria João Pinho and Patrício Soares-da-Silva

Institute of Pharmacology and Therapeutics, Faculty of Medicine, 4200-319 Porto, Portugal

Correspondence and offprint requests to: Patrício Soares-da-Silva; E-mail: psoaresdasilva@netcabo.pt

Abstract

Background. Partial renal ablation is associated with compensatory renal growth, significant azotaemia, a significant increase in fractional excretion of sodium and changes in solute transport. The present study evaluated the occurrence of adaptations in the remnant kidney, especially in renal amino acid transporters and sodium transporters and their putative role in sodium handling in the early stages (24 h and 1 week) after uninephrectomy.

Methods. Wistar rats aged 8 weeks old were submitted to renal ablation of the right kidney—Unx rats ($n = 10$). 24 hours ($n = 5$) and 1 week ($n = 5$) after surgery, rats were anesthetized and the left kidney was removed. Urinary and plasmatic levels of catecholamines, sodium, urea and creatinine were measured. Gene expression of the amino acid and sodium transporters was determined by Real-time reverse transcription PCR. Protein expression was evaluated by Western blot using specific antibodies for the amino acid and sodium transporters.

Results. Uninephrectomized (Unx) rats for 24 h showed a lower urinary excretion of L-DOPA, dopamine and DOPAC than the corresponding Sham rats, accompanied by an increase in the expression of the Na^+-K^+-ATPase protein (64% increase). Unx rats for 1 week presented a hypertrophied remnant kidney, higher urine outflow and a ∼2-fold increase in the fractional excretion of sodium. The NHE3 mRNA expression was significantly decreased in Unx rats throughout the study (∼20% decrease). LAT1 transcript and protein were consistently overexpressed at both 24 h and 1 week after uninephrectomy. In contrast, 4F2hc and LAT2 transcript abundance was lower in 24-h Unx rats than in Sham rats (a 36% decrease in both cases).

Conclusions. These results provide evidence that the renal expression of the amino acid transporters LAT1, LAT2 and 4F2hc and the sodium transporters Na^+-K^+-ATPase and NHE3 is differently regulated following unilateral nephrectomy. In conclusion, this study allowed us to characterize the renal adaptations in the early stages after uninephrectomy, which showed a combined interaction of multiple mechanisms regulating sodium homeostasis including the renal dopaminergic system, and the abundance of amino acid transporters and sodium transporters.

Keywords: LAT1; LAT2; renal dopaminergic system; renal mass reduction

Introduction

The number of renal transplantations with living donor kidneys is progressively increasing world-wide, thus increasing the necessity of detailed knowledge about the short-term and long-term risks involved in this procedure [1]. Increased blood pressure and creatinine levels, hypertension and proteinuria are associated with unilateral nephrectomy in human subjects (reviewed in [2]). However, the factors contributing to the adaptations of the remaining kidney have not been systematically evaluated.

Animal models of reduced renal mass undergo a series of adaptive mechanisms to maintain sodium homeostasis. As the population of surviving nephrons is reduced, the remaining tissue undergoes compensatory hypertrophy with marked alterations in tubular reabsorptive capacities of sodium and water [3–5]. Compensatory changes in the tubular handling of sodium include an increased excretion

© The Author [2009]. Published by Oxford University Press on behalf of ERA-EDTA. All rights reserved.
For Permissions, please e-mail: journals.permissions@oxfordjournals.org